Monthly Notices of the ROYAL ASTRONOMICAL SOCIETY

MNRAS **507,** L6–L10 (2021) https://doi.org/10.1093/mnrasl/slab082
Advance Access publication 2021 July 20

SMILE: Search for MIlli-LEnses

C. Casadio [1,2,3★] D. Blinov [1,2,4★] A. C. S. Readhead,[5] I. W. A. Browne,[6] P. N. Wilkinson,[6] T. Hovatta,[7,8] N. Mandarakas,[1,2] V. Pavlidou [1,2] K. Tassis,[1,2] H. K. Vedantham [9,10] J. A. Zensus,[3] V. Diamantopoulos,[2] K. E. Dolapsaki,[2] K. Gkimisi,[2] G. Kalaitzidakis,[2] M. Mastorakis,[2] K. Nikolaou,[2] E. Ntormousi,[1,2,11] V. Pelgrims[1,2] and K. Psarras[2]

[1]*Institute of Astrophysics, Foundation for Research and Technology – Hellas, Voutes, 7110 Heraklion, Greece*
[2]*Department of Physics, University of Crete, 71003 Heraklion, Greece*
[3]*Max-Planck-Institut für Radioastronomie, Auf dem Hügel 69, D-53121 Bonn, Germany*
[4]*Astronomy Department, St Petersburg State University, Universitetsky pr. 28, Petrodvoretz, 198504 St Petersburg, Russia*
[5]*Cahill Center for Astronomy and Astrophysics, California Institute of Technology, 1200 E California Blvd, MC 249-17, Pasadena, CA 91125, USA*
[6]*Jodrell Bank Observatory, University of Manchester, Nr. Macclesfield, Cheshire SK11 9DL, UK*
[7]*Finnish Centre for Astronomy with ESO, FI-20014, University of Turku, Finland*
[8]*Metsähovi Radio Observatory, Aalto University, Metsähovintie 114, FI-02540 Kylmälä, Finland*
[9]*Kapteyn Astronomical Institute, University of Groningen, Postbus 800, 9700 AV Groningen, The Netherlands*
[10]*Leiden Observatory, Leiden University, PO Box 9513, NL-2300 RA Leiden, the Netherlands*
[11]*Scuola Normale Superiore, Piazza dei Cavalieri 7, I-56126 Pisa, Italy*

Accepted 2021 July 13. Received 2021 July 8; in original form 2021 April 23

ABSTRACT

Dark matter (DM) haloes with masses below $\sim 10^8$ M$_\odot$, which would help to discriminate between DM models, may be detected through their gravitational effect on distant sources. The same applies to primordial black holes, considered as an alternative scenario to DM particle models. However, there is still no evidence for the existence of such objects. With the aim of finding compact objects in the mass range of $\sim 10^6$–10^9 M$_\odot$, we search for strong gravitational lenses on milliarcsec scales (<150 mas). For our search, we used the Astrogeo very long baseline interferometry (VLBI) FITS image data base – the largest publicly available data base, containing multifrequency VLBI data of 13 828 individual sources. We used the citizen science approach to visually inspect all sources in all available frequencies in search for images with multiple compact components on mas scales. At the final stage, sources were excluded based on the surface brightness preservation criterion. We obtained a sample of 40 sources that passed all steps and therefore are judged to be mas lens candidates. These sources are currently followed up with ongoing European VLBI network observations at 5 and 22 GHz. Based on spectral index measurements, we suggest that two of our candidates have a higher probability to be associated with gravitational lenses.

Key words: dark matter – gravitational lensing: strong – quasars: general – techniques: interferometric.

1 INTRODUCTION

The distribution of mass aggregates below $\sim 10^9$ M$_\odot$ is of crucial importance in structure formation and possibly also in identifying the nature of dark matter (DM). The standard cold dark matter model (CDM) predicts the formation of a larger number of DM haloes on subgalactic scales (subhaloes) than the warm dark matter model. Given that DM haloes with masses below $\sim 3 \times 10^8$ M$_\odot$ should not form galaxies (Benitez-Llambay & Frenk 2020), the only way to detect them in distant galaxies is through gravitational lensing effects on distant background sources (e.g. Vegetti et al. 2012).

Gravitational lensing occurs when light rays from a distant source are bent by the gravitational potential of a foreground mass distribution (*lens*). If the surface density of the lens is high enough (Treu 2010; Zackrisson & Riehm 2010), and if a compact background source and the lens are well aligned with the observer, multiple images of the background source will be formed. This is the case of *strong lensing*. Based on the angular scale at which multiple images form in the lens plane, strong lensing can be further divided into three regimes: *macro* (∼arcsec), *milli* [milliarcsec (mas)], and *micro* (microarcsec) lensing.

The cosmic lens all sky survey (CLASS; Browne et al. 2003; Myers et al. 2003) and Jodrell Very Large Array (VLA) astrometric survey (King et al. 1999) used the VLA to identify 20 new gravitational macro-lenses due to galactic mass lenses of $\sim 10^{11}$ M$_\odot$, and found a lensing rate of one macro-lens per 690 ± 190 radio sources observed in a complete flux density limited sample (Browne et al. 2003).

The milliarcsecond gravitational lenses or *milli-lenses* can probe different astrophysical systems. Lensed images separated by 5–100 mas are expected when the lens is a compact object (CO) with a mass between 10^6 and 10^9 M$_\odot$, i.e. a *supermassive CO*. Hence, milli-lenses can reveal dormant supermassive black holes (BHs) located at the centres of galaxies or free floating in the intergalactic space.

★ E-mail: ccasadio@ia.forth.gr(CC); blinov@ia.forth.gr(DB)

In this case, the BH splits the image formed close to the centre of mass (Mao, Witt & Koopmans 2001; Winn, Rusin & Kochanek 2004; Muller et al. 2020) into multiple images on mas scales, which are accessible to very long baseline interferometry (VLBI) observations.

Wilkinson et al. (2001) used VLBI multifrequency observations of 300 sources to search for milli-lenses with multiple-image separations in the angular range of 1.5–50 mas. Following Press & Gunn (1973), their null result allowed them to constrain the CO mass density (Ω_{CO}) for CO in the mass range of 10^6-10^8 $M_\odot$, to $\Omega_{CO} < 0.01$ (95 per cent confidence).

The very long baseline array (VLBA) has been used by Spingola et al. (2019) at 1.4 GHz in a search for milli-lenses with image separations >100 mas, corresponding to lensing mass scales $>3 \times 10^9$ $M_\odot$. In terms of mass scale, this complements the study we report here. Following Wilkinson et al. (2001), we selected a higher frequency than 1.4 GHz in order to focus on lensing of the compact cores of blazars and to reduce the confusing effects of the radio jets, which have steeper spectra than the cores. The cores we are targeting for multiple images due to lensing are much more prominent relative to the jets at 8 GHz than at 1.4 GHz.

Lately, there has been a renewed interest in the primordial black hole (PBH) scenario, partially due to the merging of an $\sim$85 $M_\odot$ BH and an $\sim$66 $M_\odot$ BH, recently detected by the LIGO/Virgo Collaboration (De Luca et al. 2021). If PBHs exist, they might be the primary constituent of DM (e.g. Clesse & García-Bellido 2018). Moreover, given the wide range of possible masses of these objects (10^{-18}–10^9 $M_\odot$; Sasaki et al. 2018) PBHs could explain the high BH masses in the above LIGO/Virgo event.

In this paper, we present a pilot search for milli-lenses with an angular separation <150 mas, which we carried out using the Astrogeo VLBI FITS image data base.[1] We used the VLBI data of all 13 828 sources, available when this study was performed. A similar study was presented by Burke-Spolaor (2011). There, the search for binary supermassive BHs using spectral index images of 3114 sources produced only one candidate. The bulk of sources in the Astrogeo VLBI FITS image data base come from dedicated astrometry programmes devoted to the completion of a radio fundamental catalogue (Petrov 2021). For this reason, Astrogeo contains mostly compact radio sources observed in two frequency bands, and one of them is usually the *X* band (8 GHz). This relatively high frequency is ideal for gravitational lens searches since at this frequency most of these sources are dominated by an unresolved flat-spectrum core, making the identification of multiple lensed images of the core straightforward.

We identify 40 milli-lens candidates, which are promising targets for follow-up observations. We additionally provide an example of such follow-up, using newly obtained European VLBI network (EVN) data, for two of our candidates. We encourage further observations of this kind for the rest of our 40 candidates.

2 SEARCH FOR LENSES

For this study, we downloaded all the UV-FITS files, with associated clean components, available at the Astrogeo VLBI FITS image data base at the time this search was performed, for a total of 13 828 individual sources. Starting from self-calibrated visibilities and using clean components, we produced new images with circular restoring beams of diameter $d = \sqrt{a_{maj} \times a_{min}}$, where a_{maj} and a_{min} are the major and minor axes of the restoring beams in the original image FITS files. In case of sources with multi-epoch observations at any particular observing band, we convolved visibilities with a median circular beam and we median stacked the multi-epoch images together, using intensity peaks to align them. Final images have a dimension of 1024 × 1024 pixels and 0.3 mas per pixel, resulting in a field of view of $\sim$307 × 307 mas.

In order to visually inspect all resulting images of all sources, we then created a web page similar, in concept, to interfaces of citizen science projects (e.g. Banfield et al. 2015). At every reload, the web page showed the final images in all available bands for a single source. Images were displayed using JS9[2] windows that allowed us to change flux density levels, dynamic range, zoom, etc. Hyperlinks to original single-epoch FITS and poscript image files were also included in the web page. At the bottom of the web page, two buttons, namely 'Lens' and 'No Lens', allowed the user to judge the source as a possible gravitational lensing candidate or not, on the basis of the visual inspection of displayed images. As a control, we also inserted, within the sample, 200 mock lens images, i.e. images displaying two separated compact components that were generated in the following way. First, we visually selected 200 random sources from the sample where only a central compact source and no secondary components within the 307 × 307 mas field of view were present at any available band. Then, we fitted the source core with a circular Gaussian function and randomly scaled its parameters to create the mock lens. The height and the standard deviation of the Gaussian were multiplied by random factors drawn from uniform distributions in the range of [0.3, 1] and [0.8, 1.2], respectively. After this, we added the corresponding mock Gaussian function to a random location in the image. If multiple bands were present, the same scaling factor was used for all of them. We repeated this procedure for all the 200 sources. In this way, the mock lens images were reproduced as double compact components with similar spectral index and surface brightness. We mixed these mock lensed objects in the data base so that they would be offered for classification by users in a random order among real sources. The mock lenses were injected into the data base in order to evaluate attentiveness of each user and roughly estimate completeness of our search. Users were instructed to select any sources with multiple compact components regardless their flux ratio, surface brightness, or separation. For this reason, we did not aim to create a set of mock lenses, whose parameters would follow physically realistic distributions. Moreover, given that the lens mass distribution is unknown and no milli-lenses have been detected so far, it may not be possible to create such a set.

The first step of the sample selection consisted in the visual inspection of the 13 828 sources through the web page interface. To complete this task, five PhD scientists and nine undergraduate Physics students from the University of Crete were involved. They were asked to mark as 'Lens' sources showing multiple compact components in at least one of the available observing bands, and as 'No Lens' the rest of sources. Considering the lack of expertise in VLBI images of active galactic nucleus for most of the participants in the search, people were asked to mark also as 'Lens' sources with some kind of extension (even core–jet structure) in case of doubt on the nature of the source itself. In this way, we sought to prevent loss of potential candidates right at the start of the search. Each source in the data base was inspected by one user and the corresponding choice was recorded. After this first step, 950 sources (excluding the mock lenses) had been catalogued as potential lenses. Among the 200 mock lenses, 8 were missed. Two specific persons together

[1] http://astrogeo.org/vlbi_images

[2] https://js9.si.edu/

were responsible for missing six out of these eight sources. Given the higher than average rate of failure, their judgments were considered unreliable. Therefore, two of the authors who are experienced VLBI researchers re-inspected all sources classified by the original two people. They recovered the mock lenses and also selected four more lens candidates in addition to the 950 previously obtained. The final result is that the number of missed mock lenses was two and hence we estimate the final loss rate of real lens candidates as ∼1 per cent (2/200).

After this first stage, a detailed visual inspection of the 954 sources was performed by CC and DB. Sources were rejected if they showed clear surface brightness or spectral index discrepancies between components, clear processing artefacts, and/or clear core–jet structures without evidence of any other unresolved bright component aside from the core. After this second stage, we were left with 128 candidates. Three more authors (AR, IB, and PW), who led the CLASS project and were therefore familiar with radio images of lenses, then examined these 128 sources, and rejected 69 more objects. Our remaining sample, after these multiple stages of visual inspections, consisted of 59 lens candidates.

Since a significant number of images come from astrometry and geodesy programmes, with poor uv coverage and short integration times, they may have artefacts and lack extended weak emission. Therefore, we decided to use a conservative approach, and finally reject sources based on the surface brightness preservation criterion; i.e. components fainter than the core should appear more compact. Since gravitational lensing preserves the surface brightness of the background source, we expect the lensed images to have all the same intrinsic brightness. In Browne et al. (2003), an apparent surface brightness ratio of ∼4 between the putative lensed images has been used as a conservative upper limit to select lens candidates within the CLASS programme. Here instead, given the wide range of image quality, we used a less stringent apparent surface brightness ratio <7 to select our final list of gravitational lens candidates, 40 in total.

3 BEST CANDIDATES AND OPTICAL COUNTERPARTS

The final 40 gravitational lens candidates that passed the multiple-stage selection are listed in Table 1. This means that all 40 sources show multiple compact components at least in one of the available frequencies and the apparent surface brightness ratio between components is <7. In Fig. 1, we show two of the milli-lens candidates as they appear in our new EVN 5 GHz observations, as an example. The completion of the remaining sources' observations and data reduction is ongoing.

If the multiple components are the putative lensed images of the same source, we expect them to have the same spectra and flux density ratio between epochs. Given the small time delays between images in milli-lenses (e.g. characteristically around 20 s for a CO of 10^7 $M_\odot$; Nemiroff et al. 2001), intrinsic variability on such short time-scales is likely to have a negligible effect on flux density ratios and spectral indices. For all but five sources (J0213+8717, J1143+1834, J1632+3547, J1653+3503, and J1805−0438), we have a contemporary observation at two different frequencies (either 8 and 4.3 GHz or 8 and 2.3 GHz) that we use to compute the spectral indices of the multiple components. We used `Difmap` (Shepherd 1997) to fit the multiple components observed in each source with circular Gaussian brightness distributions and we computed the components spectral indices α ($S_\nu \propto \nu^\alpha$) at the available frequencies. As pointed out by Spingola et al. (2019), spectral indices may be biased towards high negative values because of the combined effect of

Table 1. Best lens candidates: (1) – J2000 name; (2) and (3) – Right ascension and declination (J2000) according to NASA/IPAC Extragalactic Database.

ID	RA h:m:s	Dec. d:m:s
J0010−0740	00:10:50.60	−07:40:12.10
J0011+3443	00:11:17.01	+34:43:33.64
J0024−4202	00:24:42.99	−42:02:03.95
J0044+2858	00:44:21.55	+28:58:33.84
J0052+1633	00:52:36.17	+16:33:00.45
J0118+3810	01:18:10.14	+38:10:55.10
J0132+5211	01:32:18.92	+52:11:30.70
J0139+0824	01:39:57.16	+08:24:26.80
J0203+3041	02:03:45.36	+30:41:29.11
J0210−2213	02:10:10.06	−22:13:36.90
J0213+8717	02:13:57.85	+87:17:28.8
J0222+0952	02:22:15.61	+09:52:37.80
J0232−3422	02:32:30.03	−34:22:03.10
J0237+1116	02:37:13.59	+11:16:15.48
J0502+1626	05:02:47.39	+16:26:39.32
J0527+1743	05:27:23.21	+17:43:25.10
J0616−1957	06:16:01.57	−19:57:16.20
J0732+6023	07:32:50.97	+60:23:40.06
J0923−3435	09:23:53.88	−34:35:26.10
J1132+5100	11:32:50.39	+51:00:19.92
J1143+1834	11:43:26.07	+18:34:38.36
J1218−2159	12:18:58.82	−21:59:45.4
J1306+0341	13:06:16.00	+03:41:40.80
J1340−0335	13:40:13.30	−03:35:20.80
J1344−1739	13:44:03.42	−17:39:05.50
J1632+3547	16:32:31.25	+35:47:37.74
J1653+3503	16:53:53.16	+35:03:27.03
J1721+5207	17:21:36.26	+52:07:10.40
J1805−0438	18:05:31.12	−04:38:09.69
J2010+1513	20:10:08.20	+15:13:58.84
J2044+6649	20:44:49.19	+66:49:02.30
J2114+4036	21:14:10.01	+40:36:42.19
J2209+6442	22:09:30.49	+64:42:20.70
J2214−2521	22:14:46.39	−25:21:16.00
J2225+0841	22:25:43.48	+08:41:57.20
J2259+4037	22:59:04.04	+40:37:47.10
J2312+0919	23:12:28.07	+09:19:26.70
J2324−0058	23:24:04.62	−00:58:54.20
J2337−0622	23:37:29.19	−06:22:13.20
J2347−1856	23:47:08.63	−18:56:18.86

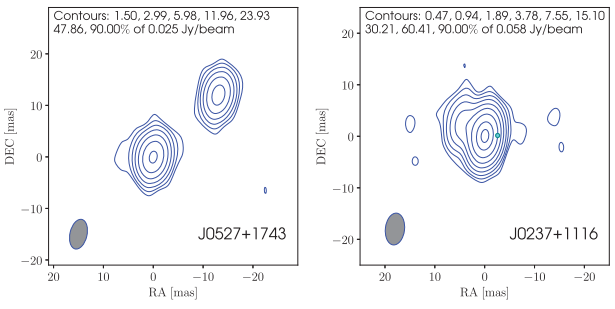

Figure 1. New EVN 5 GHz images of two milli-lens candidates, shown as example. The first contour is at 3 × rms of the map noise. Grey ellipses are the respective restoring beams. The cyan dot indicates the optical photocentre position (Kovalev et al. 2020), with error bars taken from *Gaia Early Data Release* (*EDR*) *3* that are smaller than the symbol size. In the new EVN image, J0527+1743 preserves the multicompact components structure, while J0237+1116 shows a clear core–jet structure, which differs from the image selected within our search for milli-lenses.

higher angular resolution and poorer sensitivity at high frequencies. Moreover, we cannot discard the possibility that light rays, which go through different paths to produce multiple images, cross different plasma with different absorption coefficients. This would also lead to multiple images with different spectral indices. Therefore, we use the spectral indices obtained only to suggest, among the 40 best candidates, sources that have the highest probability to be associated with gravitational lenses rather than reject candidates. These must have multiple components with similar flat ($\alpha < 0.5$) spectral indices, in order to be lensed images of a core–jet system in the background. Among the 40 candidates, the two sources which best satisfy these criteria are J0527+1743 and J2312+0919. A third promising source is J1143+1834, for which no spectral index information is available.

We also investigated the optical counterparts of the 40 lens candidates, using the publicly available optical catalogues in ALADIN SKY ATLAS. Only 15 sources have associated optical counterparts and among them only four sources (J0024−4202, J0210−2213, J2214−2521, and J2312+0919) have known redshifts.

Another important piece of information comes from the comparison between the optical and VLBI position. VLBI-*Gaia* offsets are a widely discussed topic (e.g. Kovalev, Petrov & Plavin 2017; Xu et al. 2021, and references therein) and it has been shown that such offsets can be used as a tool to distinguish between the accretion disc and jet emission regions (Plavin, Kovalev & Petrov 2019). Six sources from our sample have coordinates within 0.5 arcsec from optical sources in the *Gaia* EDR 3 (*Gaia* Collaboration 2021). However, only for two of them accurate VLBI-*Gaia* offsets are available. In J0237+1116, the *Gaia* position is shifted in the opposite direction of the extended emission in the *C* band that connects the two bright components at the *X* band, and is located 2.6 mas west of the brightest component (Kovalev et al. 2020). This may suggest that what we see in our VLBI image is a core–jet structure while the optical emission comes mostly from the accretion disc following Plavin et al. (2019). This is supported by our newly obtained EVN 5 GHz image (see Fig. 1), where the source shows a clear core–jet structure, which allows us to discard it as a lens. In J2214−2521, for which the radio position is available in the International Celestial Reference Frame (ICRF3) (Charlot et al. 2020), the VLBI-*Gaia* offset is ∼155 mas. The separation between radio components in this source is an order of magnitude smaller. The optical image from PanSTARRS that reveals the presence of an extended galaxy at a redshift (z) of 0.0868 suggests that in this case some bright optical emitting region within the galaxy may be responsible for the offset of the optical position or, an alternative scenario, the radio source is a background object, while *Gaia* measures the optical photocentre of the nearby foreground galaxy. We will further investigate VLBI-*Gaia* offsets of our lens candidates in future publication after a careful analysis of EVN phase-referencing observations.

We report below a few extra notes and considerations on some of the sources.

J0024−4202: Previously classified as a gigahertz peaked spectrum (GPS) radio galaxy (e.g. Labiano et al. 2007); the optical counterpart is located at a redshift (z) of 0.937.

J0210−2213: Classified as a GPS source (Snellen et al. 2002), the optical counterpart is located at a redshift (z) of 1.49.

J1132+5100: Located behind the galaxy cluster Abell 1314 (Vallee & Roger 1989). The different spectral indices of components A and B suggest that they are not images of each other and should be discarded. However, the peculiar location of this source, behind a galaxy cluster, is favourable for the search of gravitational lens systems.

J1143+1834: This source has been previously reported as compact symmetric object (CSO; Sokolovsky et al. 2011) and supermassive binary black hole (SBBH) candidates (Tremblay et al. 2016).

J1632+3547: Tremblay et al. (2016) discarded this source as a CSO candidate, but they still propose it as an SBBH candidate.

J1653+3503: This source has been discarded as both CSO and SBBH candidates (Tremblay et al. 2016).

J2312+0919: Associated with a Fanaroff–Riley II – high-excitation radio galaxy, 3C 456 (e.g. Macconi et al. 2020); the optical counterpart is located at a redshift (z) of 0.233.

J2347−1856: Previously classified as a CSO (Taylor & Peck 2003; Sokolovsky et al. 2011).

4 CANDIDATE CONFIRMATION

We performed a pilot search for mas gravitational lenses to probe the existence of COs in the mass range of 10^6–10^9 $M_\odot$. The possible locations and origins of such objects are different. For example, a supermassive CO could be a quiescent supermassive BH hosted within a galaxy or one of the CDM subhaloes expected to surround the host galactic CDM halo (Kravtsov 2010). In both cases, we should expect to see optical emission associated with the host galaxy in the lens plane. In the case of a free-floating CO (either a supermassive BH or a DM halo), it is possible that no optical emission is associated with the lens. Hence, the optical emission, if present, should be associated with the lensed source and, therefore, should be lensed like the radio emission. This means that, if the radio and optical are cospatial in the lensed source, the *Gaia* position is expected to be in between the putative lensed images, given the inability of *Gaia* observatory to resolve components with an angular separation lower than ∼100 mas (Lemon et al. 2017). The situation is different if the optical and radio emissions are not cospatial (e.g. Reines et al. 2020). In this case, we may still expect the optical emission being lensed, but the *Gaia* position is not expected necessarily to fall in between the putative lensed images observed at VLBI scales.

The optical counterparts of these sources will be one of the aspects to investigate in further analysis, but we mostly expect multifrequency and/or multi-epoch VLBI observations in future to be fundamental for finally confirming or rejecting the lens nature of these candidates. Since the short time delays in milli-lenses do not create delay-dependent changes in flux ratios, multi-epoch observations will help in discarding many candidates based on flux density ratio measurements between the putative lens images. Ultimately, the sources that will preserve flux density ratios despite flux density variability over epochs, and have multiple compact components with similar spectral indexes, will be tested using lens modelling to verify if the configuration and relative flux densities are compatible with a gravitational lens system.

5 DISCUSSION AND FURTHER ACTIONS

The sample of the 40 most probable milli-lens candidates is being followed up with EVN observations at 5 and 22 GHz (Project ID: EC071; PI: Casadio). Higher sensitivity 5 GHz images should help to discard core–jet structures if present, and with the addition of the 22 GHz we hope to better resolve the structure of compact components and to add more spectral information. We encourage the community to join with more follow-up observations.

Any sources that do not pass the follow-up tests and are rejected as milli-lens candidates can still be investigated as candidates for an SBBH system or a CSO. CSO and GPS radio galaxies, based on morphological and spectral classification, respectively, are thought

to be the young counterparts of extended radio sources. The radio emission in these objects mostly comes from lobes, which often have compact hotspots separated by <1 kiloparsec (Wilkinson et al. 1994). For this reason, their morphology may resemble that of a gravitational lens system on scales from mas to tens of mas. Therefore, if not confirmed as gravitational lens candidates by upcoming observations, some of our lens candidates could be investigated as CSO candidates. In the previous section, we specified the four sources that have been previously classified as either CSO or GPS. For the remaining 36 sources, no information was found. Another important application of this search is the possible discovery of SBBH systems which can also display compact components on mas scales (Taylor et al. 2007; Gitti et al. 2013).

The confirmation of any of these sources as a milli-lens would be a major discovery. On the contrary, a null result would help to constrain Ω_{CO}, as in the study of Wilkinson et al. (2001). However, in order to constrain Ω_{CO}, we need to perform such a search on a complete sample of sources. For this purpose, we selected a complete sample of sources with flux density at 8 GHz higher than 50 mJy, starting from the complete sample in CLASS (Browne et al. 2003). Sources that have not been previously observed with VLBI observations will be observed with VLBA at 4.3 and 7.6 GHz in 2020–2021 (Project ID: BR235; PI: Readhead). This complete sample of ∼5000 sources, in case of null result from the search of milli-lenses, will help us set an upper limit on Ω_{CO} with a precision of over an order of magnitude better than that in Wilkinson et al. (2001), who analysed a complete sample of 300 sources.

ACKNOWLEDGEMENTS

CC, DB, NM, V. Pelgrims, and KT acknowledge support from the European Research Council (ERC) under the European Union Horizon 2020 research and innovation program under the grant agreement number 771282. V. Pavlidou acknowledges support from the Foundation of Research and Technology - Hellas Synergy Grants Program through project MagMASim, jointly implemented by the Institute of Astrophysics and the Institute of Applied and Computational Mathematics and by the Hellenic Foundation for Research and Innovation (HFRI) under the 'First Call for H.F.R.I. Research Projects to support Faculty members and Researchers and the procurement of high-cost research equipment grant' (Project 1552 CIRCE). TH was supported by the Academy of Finland projects 317383, 320085, and 322535. We thank Fotini Bouzelou and John Kypriotakis, who also helped in the search for lens candidates. We would like to thank the MPIfR internal referee Silke Britzen for the careful reading of the manuscript. We would like also to thank Leonid Petrov for maintaining the Astrogeo VLBI FITS image data base and A. Bertarini, L. Vega Garcia, N. Corey, Y. Cui, L. Gurvits, X. He, Y. Y. Kovalev, S-S. Lee, R. Lico, E. Liuzzo, A. Marscher, S. Jorstad, C. Marvin, D. Homan, M. Lister, A. Pushkarev, E. Ros, T. Savolainen, K. Sokolovski, A. Tao, G. Taylor, A. de Witt, M. Xu, and B. Zhang for making VLBI images they produced publicly available. We found that a practice to upload VLBI images to a publicly available data base brings great benefits to the scientific community. This research has made use of ALADIN SKY ATLAS developed at CDS, Strasbourg Observatory, France (Bonnarel et al. 2000).

DATA AVAILABILITY

The FITS images and UV-FITS files underlying this article are publicly available at the Astrogeo VLBI FITS image data base (http://astrogeo.org/vlbi_images). The usage policy of the Astrogeo VLBI FITS image data base as well as the presence of unpublished material within the data base does not permit the publication of either images or source-related data obtained along with this study.

REFERENCES

Banfield J. K. et al., 2015, MNRAS, 453, 2326
Benitez-Llambay A., Frenk C., 2020, MNRAS, 498, 4887
Bonnarel F. et al., 2000, A&AS, 143, 33
Browne I. W. A. et al., 2003, MNRAS, 341, 13
Burke-Spolaor S., 2011, MNRAS, 410, 2113
Charlot P. et al., 2020, A&A, 644, A159
Clesse S., García-Bellido J., 2018, Phys. Dark Universe, 22, 137
De Luca V., Desjacques V., Franciolini G., Pani P., Riotto A., 2021, Phys. Rev. Lett., 126
Gaia Collaborationet al., 2021, A&A, 649, 20
Gitti M., Giroletti M., Giovannini G., Feretti L., Liuzzo E., 2013, A&A, 557, L14
King L. J., Browne I. W. A., Marlow D. R., Patnaik A. R., Wilkinson P. N., 1999, MNRAS, 307, 225
Kovalev Y. Y., Petrov L., Plavin A. V., 2017, A&A, 598, L1
Kovalev Y. Y., Zobnina D. I., Plavin A. V., Blinov D., 2020, MNRAS, 493, L54
Kravtsov A., 2010, Adv. Astron., 2010, 281913
Labiano A., Barthel P. D., O'Dea C. P., de Vries W. H., Pérez I., Baum S. A., 2007, A&A, 463, 97
Lemon C. A., Auger M. W., McMahon R. G., Koposov S. E., 2017, MNRAS, 472, 5023
Macconi D., Torresi E., Grandi P., Boccardi B., Vignali C., 2020, MNRAS, 493, 4355
Mao S., Witt H. J., Koopmans L. V. E., 2001, MNRAS, 323, 301
Muller S., Jaswanth S., Horellou C., Martí-Vidal I., 2020, A&A, 641, L2
Myers S. T. et al., 2003, MNRAS, 341, 1
Nemiroff R. J., Marani G. F., Norris J. P., Bonnell J. T., 2001, Phys. Rev. Lett., 86, 580
Petrov L., 2021, AJ, 161, 14
Plavin A. V., Kovalev Y. Y., Petrov L. Y., 2019, ApJ, 871, 143
Press W. H., Gunn J. E., 1973, ApJ, 185, 397
Reines A. E., Condon J. J., Darling J., Greene J. E., 2020, ApJ, 888, 36
Sasaki M., Suyama T., Tanaka T., Yokoyama S., 2018, Class. Quantum Gravity, 35, 063001
Shepherd M., 1997, in Hunt G., Payne H. E., eds, ASP Conf. Ser. Vol. 125, Astronomical Data Analysis Software and Systems VI. Astron. Soc. Pac., San Francisco, p. 77
Snellen I. A. G., Lehnert M. D., Bremer M. N., Schilizzi R. T., 2002, MNRAS, 337, 981
Sokolovsky K. V., Kovalev Y. Y., Pushkarev A. B., Mimica P., Perucho M., 2011, A&A, 535, A24
Spingola C., McKean J. P., Lee M., Deller A., Moldon J., 2019, MNRAS, 483, 2125
Taylor G. B., Peck A. B., 2003, ApJ, 597, 157
Taylor G. B., Rodriguez C., Zavala R. T., Peck A. B., Pollack L. K., Romani R. W., 2007, in Karas V., Matt G., eds, Black Holes from Stars to Galaxies – Across the Range of Masses. Vol. 238, p. 269
Tremblay S. E., Taylor G. B., Ortiz A. A., Tremblay C. D., Helmboldt J. F., Romani R. W., 2016, MNRAS, 459, 820
Treu T., 2010, ARA&A, 48, 87
Vallee J. P., Roger R. S., 1989, A&AS, 77, 31
Vegetti S., Lagattuta D. J., McKean J. P., Auger M. W., Fassnacht C. D., Koopmans L. V. E., 2012, Nature, 481, 341
Wilkinson P. N., Polatidis A. G., Readhead A. C. S., Xu W., Pearson T. J., 1994, ApJ, 432, L87
Wilkinson P. N. et al., 2001, Phys. Rev. Lett., 86, 584
Winn J. N., Rusin D., Kochanek C. S., 2004, Nature, 427, 613
Xu M. H., Lunz S., Anderson J. M., Savolainen T., Zubko N., Schuh H., 2021, A&A, 647, A189
Zackrisson E., Riehm T., 2010, Adv. Astron., 2010, 478910

This paper has been typeset from a TEX/LATEX file prepared by the author.